Chapter 10 Introduction to Thermoelectricity

Department of Applied Physics, Waseda University Ichiro Terasaki

10.1 Brief introduction to thermoelectrics

In this chapter, we will review the current status of thermoelectrics --- the energy-conversion technology using thermoelectricity (Mahan 1998). Since thermoelectrics is a direct energy-conversion technology by electrons in solids, it possesses various advantages in harmony with our environments. We will begin with thermoelectric phenomena in solids, and briefly review thermoelectric devices and their applications in this section. Next in 10.2, we will discuss the thermodynamics of the thermoelectric devices, and derive a characteristic parameter called "figure of merit". In 10.3, we will elaborate on the microscopic picture of thermoelectric materials. Then we will review conventional thermoelectric materials in 10.4, and thermoelectric oxides in 10.5. Finally we will summarize this chapter, and briefly comment on future prospects.

10.1.1 the Seebeck effect and the Peltier effect

An electron in solids is an elementary particle with a negative charge of e, and carries electric current. Since an enormous number of electrons are at thermal equilibrium in solids, they also carry heat and entropy. Thus in the presence of temperature gradient, they can flow from a hot side to a cold side to cause an electric current. This implies a coupling between thermal and electrical phenomena, which is called thermoelectric effects.

The Seebeck effect and the Peltier effect are predominant thermoelectric effects. The Seebeck effect is a phenomenon that voltage (V) is induced in proportion to applied temperature gradient (ΔT), expressed as

$$V = S\Delta T, \qquad (1)$$

where S is called the Seebeck coefficient (thermoelectric power, or thermopower). The Peltier effect is a phenomenon that the heat absorption/emission (Q) is induced at the junctions to the leads by the applied current (I), expressed as

$$Q = \Pi I, \qquad (2)$$

where Π is the Peltier coefficient. This is the reverse process to the Seebeck effect. According to the Onsagar relation, S and Π satisfy the relation as

$$\Pi = ST. \qquad (3)$$

In the presence of the coupling between thermal and electrical phenomena, it is, in principle, possible to convert heat into electric energy, and vice versa. Such a energy-conversion technology is called thermoelectrics. Since this energy conversion is done by electrons in solids, we can make full use of solids. First, the thermoelectric device has no moving part, and is operated without maintenance. Secondly, it produces no waste matter through conversion process. Thirdly, it can be processed at a micro/nano size, and can be implemented into electronic devices.

10.1.2 Thermoelectric device and its applications

Using the Peltier effect, the thermoelectric device can cool materials. It should be emphasized that thermoelectric cooling does not need any exchange media such as a freon gas, which can be a good alternative for a freon-gas refrigerator. Another advantage is that heating and cooling are quickly changed by changing the applied current direction. Thus thermoelectric refrigerator can also be a keep-warm container. Using this feature, the device can control temperature to be some value below room temperature, which is used for a wine cellar.

Using the Seebeck effect, thermal energy (heat) can be converted into electric energy, which is called thermoelectric power generation. Figure 10.1 shows the schematic picture of the thermoelectric power generation. When the left side of the sample is heated, the thermoelectric voltage is induced in proportion to

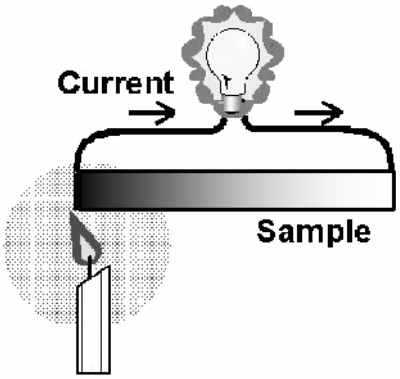

Figure 10.1 Schematic picture of thermoelectric power generation.

the temperature difference. If a load is connected to the sample, the electric power is consumed at the load. Here the thermoelectric material acts as a kind of battery, where the thermoelectric power corresponds to the electro-motive force, and the resistivity corresponds to the internal resistance. Advantages of thermoelectric power generation are (i) electric power source without maintenance, (ii) energy recovery from waist heat, and (iii) long operating lifetime. Recently, there increase pressing needs to recover energy from exhaust gas of automobiles, and many researchers and engineers have tried to make a thermoelectric power generator attached with a car engine.

10.2. Thermodynamics of thermoelectric device

10.2.1 Inequilibrium thermodynamics

Quite generally, the electric current density $\mathbf{j}$ (particle flow) and the thermal current density $\mathbf{q}$ are written as functions of the gradient of chemical potential $\nabla\mu$ and the gradient of temperature $\nabla(1/T)$ as

$$-\mathbf{j} = L_{11}\frac{1}{T}\nabla\mu + L_{12}\nabla\frac{1}{T} \qquad (4)$$

$$\mathbf{q} = L_{21}\frac{1}{T}\nabla\mu + L_{22}\nabla\frac{1}{T} \qquad (5)$$

where L_{ij}'s are transport parameters (Callen 1985).

The chemical potential consists of an electrostatic part $\mu_e = eV$ and a chemical part μ_c. Then the electric field is given as

$$\mathbf{E} = -\nabla V = -\frac{1}{e}\nabla(\mu - \mu_c). \qquad (6)$$

However, $\nabla\mu_c$ cannot be observed separately in real experiments, and is considered to be included in the observed $\mathbf{E}$ hereafter (Ashcroft and Mermin 1976).

Then the above equations are identical to the Boltzman transport equations (see 3.2) given as

$$\mathbf{j} = \sigma\mathbf{E} + S\sigma\nabla(-T) \qquad (7)$$

$$\mathbf{q} = ST\sigma\mathbf{E} + \kappa'\nabla(-T) \qquad (8)$$

where σ the conductivity, and κ' is the thermal conductivity for $\mathbf{j} \neq 0$. Then, for $\nabla T = 0$, we can eliminate the electric field term from Eqs. (7) (8), and obtain

$$\frac{\mathbf{q}}{T} = S\,\mathbf{j}. \qquad (9)$$

Since the left hand side is the entropy current density, we can say that the thermopower S is equivalent to the ratio of the entropy current to the electric current, or is equivalent to entropy per carrier.

10.2.2 Heat balance equation

Figure 10.2(a) shows a schematic picture of a thermoelectric cooling device, where R, S and K are the net resistance, thermopower, and thermal conductance of the device, respectively. For simplicity, let us consider that all the parameters of the device are independent of temperature.

In the cold side, the pumped heat Q_C is expressed as

$$Q_C = ST_cI - \frac{1}{2}RI^2 - K\Delta T, \qquad (10)$$

where the second term is the Joule heat in the sample (for simplicity, we assume that a half of the heat goes to each side), and the third term is the backflow of the

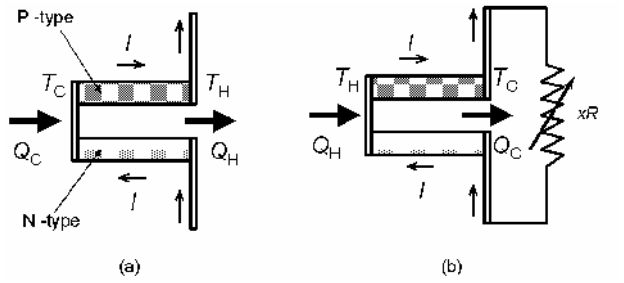

Figure 10.2 (a) Themoelectric power generator and (b) thermoelectric cooling device.

thermal current. Similarly, at the hot side, the emitted heat Q_H is expressed as

$$Q_H = ST_H I + \frac{1}{2}RI^2 - K\Delta T . \qquad (11)$$

Thus the net work is given as

$$W = Q_H - Q_C = (S\Delta T + IR)I .$$

Figure 10.2(b) shows a schematic picture of the thermoelectric power generator. As is similar to the case of the thermoelectric cooling device, the heat balance at the hot and cold sides are given as

$$Q_H = ST_H I - \frac{1}{2}RI^2 + K\Delta T . \qquad (12)$$

$$Q_C = ST_C I + \frac{1}{2}RI^2 + K\Delta T \qquad (13)$$

By connecting an external load $R_{ext} = xR$, we get the current $I = S\Delta T/(1+x)R$. Then the output power P is equal to

$$P = IV = \frac{(S\Delta T)^2}{R}\frac{x}{(1+x)^2}, \qquad (14)$$

which takes a maximum $P_{\max} = (S\Delta T)^2/4R$ at $x = 1$. Since $P_{\max}$ is determined by $S^2\sigma = S^2/\rho$ (ρ is the resistivity), $S^2\sigma$ is called the power factor.

10.2.3 Figure of merit and conversion efficiency

Let us estimate the maximum heat absorption of the cooling device for constant T_H and T_C. Then a necessary condition $dQ_C/dI = 0$ gives the optimum current $I_0 = ST_C/R$. By putting I_0 into Eq. (10), we get

$$Q_C{}^{\max} = \frac{S^2T_C{}^2}{2R} - K\Delta T = K\left(\frac{S^2T_C{}^2}{2RK} - \Delta T\right) \qquad (15)$$

Then we define the figure of merit Z as

$$Z = \frac{S^2}{RK} = \frac{S^2}{\rho\kappa}, \qquad (16)$$

and rewrite $Q_C{}^{\max}$ as

$$Q_C{}^{\max} = K\left(\frac{1}{2}ZT_C{}^2 - \Delta T\right). \qquad (17)$$

Thus the maximum heat absorption is directly proportional to Z (or the power factor) for $\Delta T = 0$.

Next we will evaluate the lowest achievable temperature T_{C0} for constant Q_C and T_H. A necessary condition $dT_C/dI = 0$ gives the optimum current $I_1 = ST_{C0}/R$. By putting I_1 into Eq. (10), we get

$$\Delta T = \frac{S^2 T_{C0}{}^2}{2KR} - \frac{Q_C}{K} = \frac{1}{2} Z T_{C0}{}^2 - \frac{Q_C}{K} \qquad (18)$$

and the maximum temperature difference (i.e. lowest achievable temperature) is again directly proportional to Z for $Q_C = 0$.

Thirdly, we will discuss the maximum efficiency. The energy conversion efficiency for a cooling device is characterized by the coefficient of performance (COP) ϕ defined as

$$\phi \equiv \frac{Q_C}{W} = \frac{Q_C}{Q_H - Q_C} = \frac{ST_C I - RI^2/2 - K\Delta T}{(S\Delta T + RI)I} . \qquad (19)$$

Taking $d\phi / dI = 0$, we obtain the optimized current I_2 as

$$I_2 = \frac{S\Delta T}{R(\sqrt{1+Z\overline{T}} - 1)}, \qquad (20)$$

where $\overline{T} = (T_C + T_H)/2$. By putting I_2 into ϕ, we get

$$\phi_{\max} = \frac{T_C\sqrt{1+Z\overline{T}} - T_H}{\Delta T(\sqrt{1+Z\overline{T}} + 1)} \qquad (21)$$

after some calculations. For the power generation, the efficiency η is given as

$$\eta \equiv \frac{W}{Q_H} = \frac{IV}{ST_H I - RI^2/2 + K\Delta T} = \frac{x\Delta T}{(1+x)\overline{T} + (1+x)^2/Z + x\Delta T/2} . \qquad (22)$$

By taking $d\eta / dx = 0$, we get the maximum efficiency is

$$\eta_{\max} = \frac{\Delta T(\sqrt{Z\overline{T}+1} - 1)}{T_H\sqrt{Z\overline{T}+1} + T_C} . \qquad (23)$$

We can take some notes on the above results. First,

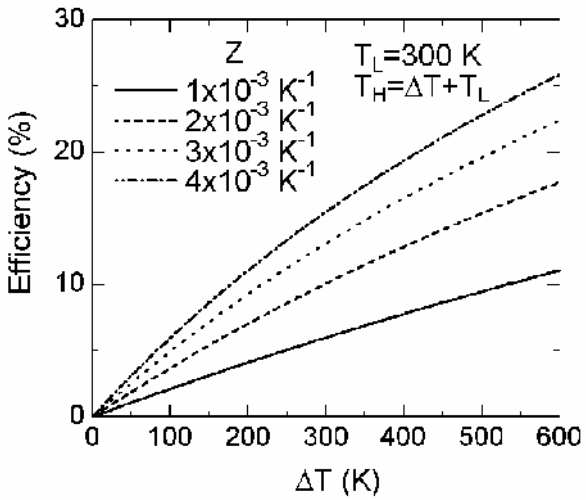

Figure 10.3 Energy conversion efficiency plotted as a function of ZT.

$\phi_{\max}$ given by Eq. (21) and $\eta_{\max}$ given by Eq. (23) are reduced to the Carnot efficiency as $ZT \to \infty$. This is reasonable, because thermoelectric energy conversion is a conversion through the electron transport, which is an irreversible process accompanying the Joule heat. Second, as shown in Figure 10.3, the efficiency η is larger for larger ZT and ΔT. Considering that the conversion efficiency of a solar battery is 10-15 %, we think that a similar η is expected for practical use, which corresponds to $Z > 3\text{x}10^{-3}$ K^{-1} and ΔT >300 K. This means that ZT =1.8 at 600 K is necessary. Thirdly, COP of a commercial refrigerator is 1.2-1.3, which corresponds to ZT =3-4. Thus much improvement in ZT is needed to replace a freon-gas refrigerator.

10.3 Microscopic theory of thermoelectric phenomena

10.3.1 The Boltzmann theory

One-electron states in a periodic potential are exactly solved, and the solution is known as the Bloch function. The Bloch function has a wave number $\mathbf{k}$ (crystal momentum) as a well-defined quantum number, and its energy $\varepsilon = \varepsilon(\mathbf{k})$ is written as a function of $\mathbf{k}$ (band dispersion relation).

To recover a particle picture, we make a wave packet

from the Bloch functions. Then the velocity of the particle is given as the group velocity of the wave as

$$\mathbf{v}_\mathbf{k} = \frac{1}{\hbar}\nabla_k \varepsilon(\mathbf{k}) = \frac{1}{\hbar}\left(\frac{\partial\varepsilon}{\partial k_x}, \frac{\partial\varepsilon}{\partial k_y}, \frac{\partial\varepsilon}{\partial k_z}\right). \quad (24)$$

To keep the particle picture, every wave constituting the wave packet should satisfy the relation of $\hbar\mathbf{k} = m\mathbf{v}_\mathbf{k}$ with a constant value of m. Then we get $m\Delta\mathbf{v}_\mathbf{k} = \hbar\Delta\mathbf{k}$, and the effective mass (the inverse of the effective mass tensor) in a solid is given as

$$\frac{1}{m_{ij}} = \frac{1}{\hbar}\frac{\partial v_{ki}}{\partial k_j} = \frac{1}{\hbar^2}\frac{\partial^2\varepsilon}{\partial k_i \partial k_j}. \quad (25)$$

Thus the electron in a solid behaves like a charged particle with the charge e, the mass m and the velocity $\mathbf{v}_\mathbf{k}$.

Since electrons are fermions, they obey the Fermi-Dirac distribution f_0. Then the electric current density and the thermal current density are written as

$$\mathbf{j} = \frac{1}{4\pi^3}\int e v_\mathbf{k} f_\mathbf{k} d^3k \quad (26)$$

$$\mathbf{q} = \frac{1}{4\pi^3}\int (\varepsilon(\mathrm{k}) - \mu) v_\mathbf{k} f_\mathbf{k} d^3k \quad (27)$$

where $f_\mathbf{k}$ is the distribution function at an inequilibrium state. $f_\mathbf{k}$ is given as a solution of the Boltzmann equation written as

$$\mathbf{v}_\mathbf{k}\cdot\nabla f_\mathbf{k} + \frac{e}{\hbar}\mathbf{E}\cdot\nabla_\mathbf{k} f_\mathbf{k} = \left.\frac{\partial f_\mathbf{k}}{\partial t}\right|_{\text{scattering}} \quad (28)$$

where the right hand side is the scattering term.

In the case of weak perturbation, we can linearize $f_\mathbf{k}$ as $f_\mathbf{k} = f_0 + g_\mathbf{k}$. We further assume the relaxation-time approximation to introduce the relaxation time τ as

$$\left.\frac{\partial f_\mathbf{k}}{\partial t}\right|_{\text{scattering}} = -\frac{1}{\tau} g_\mathbf{k}. \quad (29)$$

Eventually we get

$$g_\mathbf{k} = \left(-\frac{\partial f_0}{\partial\varepsilon}\right)_{\varepsilon(k)=\varepsilon} \mathbf{v}_\mathbf{k}\tau\left\{e\mathbf{E} + \frac{\varepsilon(\mathbf{k})-\mu}{T}(-\nabla T)\right\}. \quad (30)$$

Substituting this to Eqs. (26) (27), we obtain

$$\mathbf{j} = e^2 K_0 \mathbf{E} + \frac{e}{T} K_1(-\nabla T) \quad (31)$$

$$\mathbf{q} = eK_1\mathbf{E} + \frac{1}{T}K_2(-\nabla T) \quad (32)$$

where K_n is

$$K_n = \frac{1}{4\pi^3}\int\left(-\frac{\partial f_0}{\partial\varepsilon}\right)_{\varepsilon(k)=\varepsilon} \mathbf{v}_\mathbf{k}\mathbf{v}_\mathbf{k}\tau(\varepsilon(\mathbf{k})-\mu)^n d^3k. \quad (33)$$

Note that K_n is a second-rank tensor through $\mathbf{v}_\mathbf{k}\mathbf{v}_\mathbf{k}$, in general. Also note that Eqs. (31) (32) are identical to Eqs. (7) (8), and Onsagar's relation given in Eq. (3) is readily satisfied. It is reduced to a scalar in the cubic symmetry, and the conductivity and the thermopower are given as

$$\sigma = e^2 K_0 = \frac{1}{4\pi^3}\int\left(-\frac{\partial f_0}{\partial\varepsilon}\right)_{\varepsilon(k)=\varepsilon} {v_\mathbf{k}}^2\tau\, d^3k. \quad (34)$$

$$S = \frac{1}{eT}\frac{K_1}{K_0} = \frac{1}{eT}\frac{\int\left(-\frac{\partial f_0}{\partial\varepsilon}\right)_{\varepsilon(k)=\varepsilon} {v_\mathbf{k}}^2\tau(\varepsilon(\mathbf{k})-\mu)d^3k}{\int\left(-\frac{\partial f_0}{\partial\varepsilon}\right)_{\varepsilon(k)=\varepsilon} {v_\mathbf{k}}^2\tau\, d^3k} \quad (35)$$

The thermal conductivity is given as $\kappa' = K_2/T$ for

$\mathbf{j} \neq 0$, but the electron thermal conductivity is always measured for $\mathbf{j} = 0$. Thus, by substituting $\mathbf{E} = S\nabla T$ (from Eq. (9)) to Eq. (8), we get

$$\mathbf{q} = S^2\sigma T\nabla T + \kappa'(-\nabla T) = \kappa'(1 - S^2\sigma/\kappa')(-\nabla T) \quad , \qquad (36)$$

and the thermal conductivity observed in real situations κ is

$$\kappa = \kappa'\left(1 - \frac{S^2\sigma T}{\kappa'}\right). \qquad (37)$$

The second term corresponds to ZT for $\mathbf{j} \neq 0$. This is usually large in thermoelectric materials, and effectively reduces the real thermal conductivity given in Eq. (37).

10.3.2 Asymptotic forms of thermopower

Let us discuss thermopower of a metal intuitively. Consider a metal rod subject to a temperature gradient, as shown in Fig. 10.4. Suppose the temperature at one side is T_1, and the temperature at the other side is T_2 ($T_1 > T_2$). Since the average electron velocity is larger at T_1, electrons begin to diffuse from the side at T_1 to the side at T_2. Owing to the charge neutrality, the side at T_1 is positively charged, whereas the side at T_2 is negatively charged. This implies that the metal rod behaves like a capacitor in the temperature gradient, which is the origin of the thermoelectric voltage $V_{\rm th}$. In a steady state,

$$\mu(T_1) + eV_{th}(T_1) = \mu(T_2) + eV_{th}(T_2) \qquad (38)$$

is realized, where $\mu(T)$ is the chemical potential at temperature T. In the limit of $T_1 \to T_2$, the thermopower S (= d$V_{\rm th}$/dT) is written as

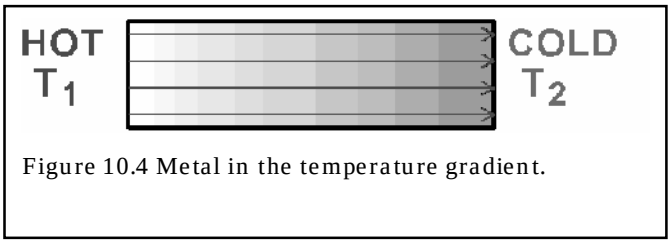

Figure 10.4 Metal in the temperature gradient.

$$S = -\frac{1}{e}\frac{\partial\mu}{\partial T} \qquad (39)$$

This equation means that the thermopower is the specific heat per carrier. This should be compared with Eq. (9).

Eq. (39) is based on a semi-classical picture, where the electrons can move "smoothly" from edge to edge like a classical particle. A complementary picture is seen in the high-temperature limit, where the transfer energy is much smaller than the thermal energy. From Eq. (35), the thermopower is written as

$$S = \frac{1}{eT}\frac{\int e^2\varepsilon_k v_k^2\tau\left(-\frac{\partial f_0}{\partial\varepsilon}\right)_{\varepsilon=\varepsilon(\mathbf{k})} d^3k}{\int e^2 v_k^2\tau\left(-\frac{\partial f_0}{\partial\varepsilon}\right)_{\varepsilon=\varepsilon(\mathbf{k})} d^3k} - \frac{\mu}{eT} \qquad (40)$$

The first term of the right hand side of Eq. (40) is of the order of $\langle\varepsilon_k\rangle/eT$, and goes to zero as $T \to \infty$.

On the contrary, the second term is rewritten with the entropy s as an identity of thermodynamics as

$$-\frac{\mu}{T} = \left(\frac{\partial s}{\partial N}\right)_{E,V} \qquad (41)$$

Thus the thermopower is associated with the entropy per carrier, which is called the Heikes formula written as

$$S = -\frac{k_B}{e}\frac{\partial \log g}{\partial N} \qquad (42)$$

where g is the total number of configurations (Chaikin and Beni 1976).

The Mott formula is perhaps most frequently used for the thermopower in metals. Eq. (35) can be associated with Eq. (34), when Fermi energy E_F is much higher than the thermal energy k_BT. By expanding the Fermi-Dirac distribution function in series of k_BT/E_F, we obtain

$$K_1 = \frac{\pi^2}{3} k_B^2 T^2 \left[\frac{\partial K_0}{\partial E} \right]_{E=\mu}, \qquad (43)$$

and the thermopower is associated with the logarithmic derivative of σ as

$$S = \frac{\pi^2}{3} \frac{k_B^2 T}{e} \left[\frac{\partial \log \sigma(E)}{\partial E} \right]_{E=\mu}, \qquad (44)$$

which is known as the Mott formula. It should be emphasized that the conductivity-like function $\sigma(E)$ in Eq. (44) is a conductivity that a metal would show, if its Fermi energy were equal to E. Do not forget that $\sigma(E)$ cannot be observed in real experiments. Thus the Mott formula should be very carefully applied for analyses of real experiments (Ashcroft and Mermin 1976).

10.4 Thermoelectric materials

10.4.1 Conventional thermoelectric materials

Thermoelectric materials so far used for practical applications are Bi_2Te_3, PbTe, and $Si_{1-x}Ge_x$. N-type BiSb is superior at low temperatures, but has no p-type counterpart. Figure 10.5 shows ZT for various thermoelectric materials. Bi_2Te_3 shows the highest performance near room temperature, and used for cooling applications such as Peltier coolers commercially available. PbTe shows the highest performance near 500-600 K, and $Si_{1-x}Ge_x$ is superior above 1000 K.

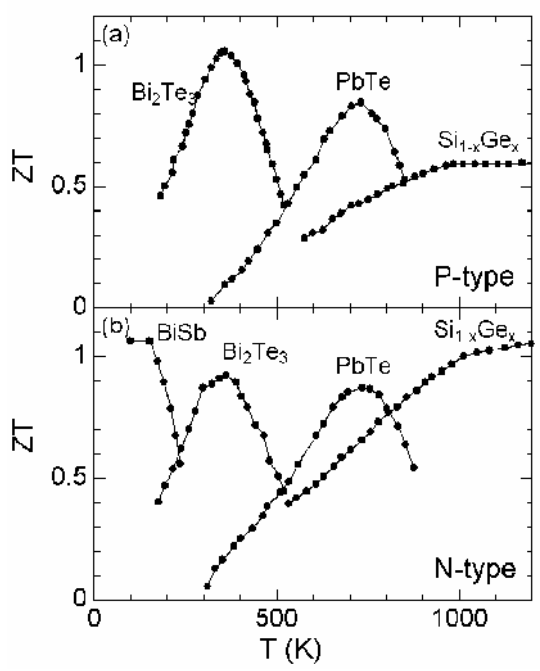

Figure 10.5 ZT for various thermoelectric materials.

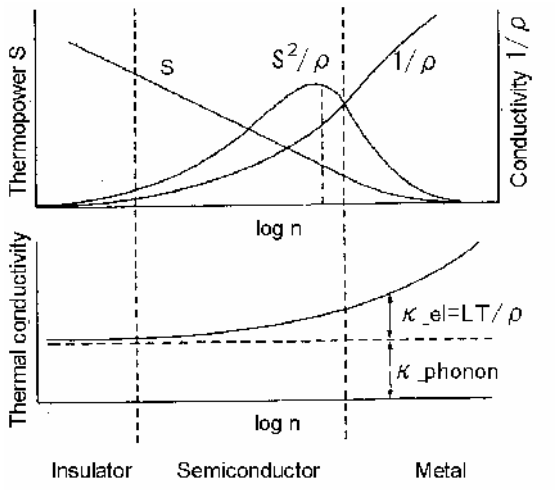

Figure 10.6 Thermoelectric parameters as a function of temperature.

The conventional thermoelectric materials are degenerate semiconductors of high mobility. Figure 10.6 shows a schematic figure of the conductivity σ, the thermopower S, the thermal conductivity κ and the power factor $S^2\sigma$ as a function of carrier concentration n (Mahan 1998). Here a simple parabolic band is assumed, and the electron-electron and electron-phonon interactions are neglected. As is seen in this figure, the thermopower decreases with n, whereas the conductivity increases with n. Then $S^2\sigma$ takes a maximum at an optimal carrier concentration n_0, below which the conductivity is too low, and above which the thermopower is too small. Assuming the Boltzmann distribution instead of the Fermi-Dirac distribution, one can evaluate that the optimum concentration is around 10^{19}-10^{20} cm^{-3}, which is close to n of a degenerate semiconductor. Since the conductivity is expressed as $\sigma = ne\mu$, the only way to maximize σ for $n = n_0$ is to maximize

Table 1 Thermoelectric parameters of conventional thermoelectric materials

	Temperature for maximum ZT (K)	Effective mass	Mobility (m^2/Vs)	Lattice thermal conductivity (W/mK)	ZT
Bi_2Te_3	300	0.2	0.12	1.5	1.3
PbTe	650	0.05	0.17	1.8	1.1
$Si_{1-x}Ge_x$	1100	1.06	0.01	4.0	1.3

the mobility μ.

As shown in Fig. 10.6, κ consists of the lattice part $\kappa_{lattice}$ and the electron part κ_{el}. Near $n = n_0$, the former part is dominant, and to maximize the figure of merit Z is to minimize $\kappa_{lattice}$ remaining $S^2\sigma$ intact. In the lowest order approximation, $\kappa_{lattice}$ is expressed as (Ashcroft and Mermin 1976)

$$\kappa_{lattice} = \frac{1}{3} C_L v_s \ell_{ph}, \qquad (45)$$

where C_L the lattice specific heat, v_s the sound velocity, and ℓ_{ph} is the phonon mean free path. Then, a material containing heavy elements (giving small v_s), solid solutions (giving short ℓ_{ph}), and many atoms in a unit cell (giving small C_L) can be a good candidate.

Mahan (1989) has suggested a microscopic parameter for good thermoelectric materials called "the B-factor" given as

$$B = \left(\frac{2mk_BT}{\pi\hbar^2} \right)^{\frac{3}{2}} \frac{\mu}{\kappa_{lattice}} \propto m^{\frac{3}{2}} \frac{\mu}{\kappa_{lattice}}. \qquad (46)$$

Note that m, μ and $\kappa_{lattice}$ are independent parameters, whereas S, ρ and κ are not. Accordingly, a degenerate semiconductor with heavier effective mass, higher mobility, and lower lattice conductivity is extensively searched. Table 1 lists the thermoelectric parameters of the conventional thermoelectric materials (Mahan 1998). σ, S and κ are around 1-2m Ω cm, 150-200 μ V/K, and 15-25 mW/cmK, respectively. The B-factor is around 0.3-0.4, which is significantly larger than that of other semiconductors.

10.4.2 Filled skutterudite compound

Since the discovery of Bi_2Te_3 in mid 50's, thermoelectric materials were extensively searched in binary systems. In fact, many promising materials were found through the research, but ZT did not exceed unity. Filled skutterudite $Ce_xFe_3CoSb_{12}$ is the first unambiguous example whose ZT exceeds unity, and is going to use for thermoelectric power generation of next generation (Sales 1997).

Figure 10.7(a) shows the crystal structure of the skutterudite $CoSb_3$. The unit cell of cubic symmetry consists of the eight sub cells whose corners are occupied by Co atoms. Six sub cells out of the eight are filled with Sb plackets, forming the valence band. According to the band calculation, $CoSb_3$ is a narrow-gap semiconductor with an indirect gap of 0.5 eV, which is favorable for a thermoelectric material. In fact, the hole mobility of $CoSb_3$ exceeds 2000

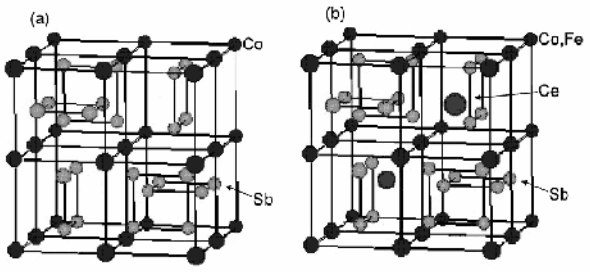

Figure 10.7 Crystal structures of skutterudite and filled

cm^2/Vs at 300 K, which is much higher than that for Bi_2Te_3 (Caillat 1996).

Figure 10.7(b) shows the crystal structure of the skutterudite $CeFe_3CoSb_{12}$. In the two vacant sub cells of the skutterudite, two Ce ions are filled. In order to compensate the charge valance, six Fe atoms are substituted for the eight Co sites, because Ce usually exists as trivalent. The most remarkable feature of this compound is that "filled" Ce ions reduce the lattice thermal conductivity several times lower than that for an unfilled skutterudite $CoSb_3$. Ce ions are weakly bound in an oversized atomic cage so that they will vibrate independently from the other atoms to cause large local vibrations. This vibration and the atom in the cage are named "rattling" and "rattler", respectively. As a result, the phonon mean free path can be as short as the lattice parameters. Namely this compound has a poor thermal conduction like a glass and a good electric conduction like a crystal, which is called "an electron crystal and a phonon glass" assumed by Slack (1995).

Figure 10.8 shows how the rattlers reduce the lattice thermal conductivity (Sales 1997). κ of $CoSb_3$ is one order of magnitude higher than κ of Bi_2Te_3, which means that Z of $CoSb_3$ is much smaller. In the filled skutterudite, however, κ is drastically reduced, and the lattice thermal conductivity is nearly the same value of SiO_2 glass. This has been a piece of evidence for phonon glass, but in the writer's opinion, it should be carefully examined whether or not the reduction of κ comes only from rattling. The filled Ce ions induce the high carrier density of the order of 10^{21} cm^{-3}, which seriously suppresses the phonon mean free path through the electron-phonon interaction. Also, the lowest κ is realized in a Ce deficient sample, and thus disorder also significantly affects the reduction of κ. In fact, κ is also dramatically reduced upon solid solutions in $CoSb_3$ (Anno and Matsubara 2000). Nevertheless, the concepts of rattling and phonon glass have been a strong driving force for thermoelectric-material search in recent years. Accordingly many promising materials, such as $Sr_6Ga_{16}Ge_{30}$ (Nolas 1998) and $CsBi_4Te_6$ (Chung 2000), have been synthesized and identified.

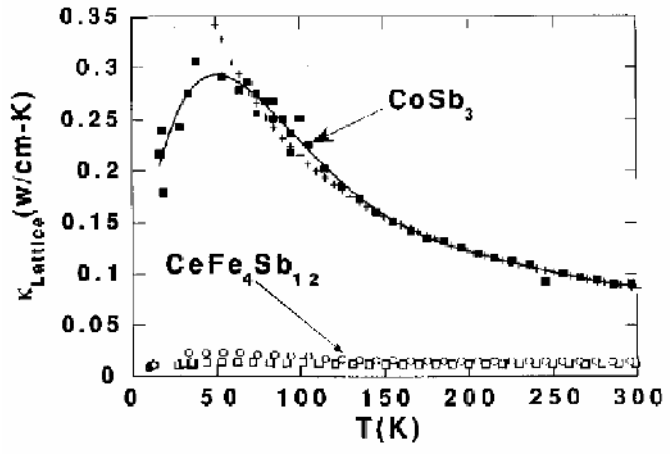

Figure 10.8 Effect of rattling.

10.5 Oxide thermoelectrics

10.5.1 Layered Co oxides

As mentioned in the previous section, the state-of-the-art thermoelectric materials are Bi_2Te_3, PbTe, and $Si_{1-x}Ge_x$, all of which are degenerate semiconductor of high mobility. Since Te is scarce in earth, toxic, and volatile at high temperature, the application of Bi_2Te_3 and PbTe has been limited. By contrast, oxide is chemically stable at high temperature in air, and thus oxide thermoelectrics is expected to use in much wider area. However, most of oxide semiconductors show very low mobility, and has been thought to be out of the question.

Since we discovered the large thermopower and the low resistivity in a $NaCo_2O_4$ single crystal (Terasaki 1997), we have proposed that some kinds of oxides can be a thermoelectric material (Koumoto 2002). Fujita et al. (2001) have succeeded in measuring the thermal conductivity of a $NaCo_2O_4$ single crystal, and found that ZT exceeds unity at 800 K. These results strongly suggest that $NaCo_2O_4$ is a promising candidate for a thermoelectric oxide. Another fascination of $NaCo_2O_4$ is existence of various related oxides. Following $NaCo_2O_4$, $Ca_3Co_4O_9$ (Funahashi and

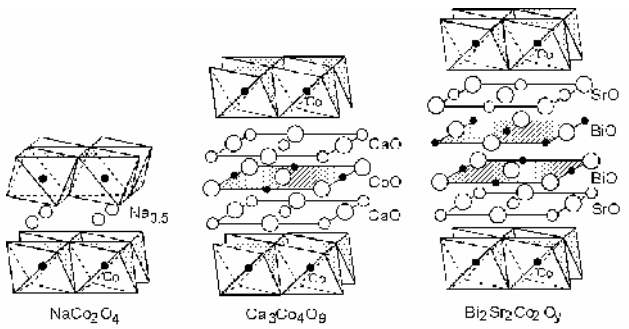

Figure 10.9 Crystal structures of the layered cobalt oxides.

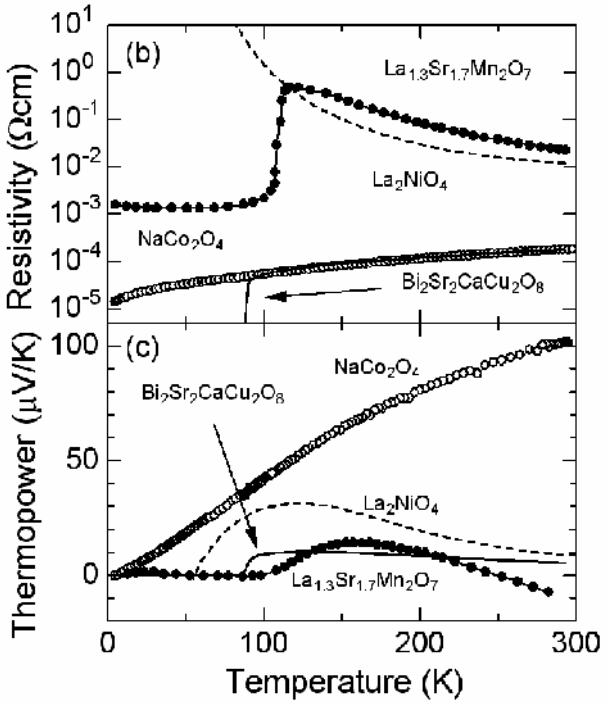

Figure 10.10 Thermoelectric properties of layered transition-metal oxides.

Mastubara 2000, Shikano and Funahashi 2003), $(Bi,Pb)_2Sr_2Co_2O_8$ (Funahashi and Mastubara 2001), $TlSr_2Co_2O_y$ (Hebert 2001), and $(Hg,Pb)Sr_2Co_2O_y$ (Maignan 2002) have been found to show good thermoelectric performance. Some single crystals show $ZT > 1$ at 1000 K. As shown in Fig. 10.9, the CdI_2-type hexagonal CoO_2 layer is common to these cobalt oxides, which reminds us of the CuO_2 plane in high-T_c superconductors (Tokura and Arima 1990). Thus the hexagonal CoO_2 layer should be a key ingredient for the unusually high thermoelectric performance of the layered Co oxides.

Not all the transition-metal oxides can be a good thermoelectric material. Figure 10.10 shows the resistivity and the thermopower of various layered transition-metal oxides. The layered Co oxide $NaCo_2O_4$ shows as low resistivity as the layered Cu oxide $Bi_2Sr_2CaCu_2O_8$ (one of high-T_c superconductors), whereas the layered Ni and Mn oxides show hopelessly high resistivity. For thermopower, the difference between the Co oxide and the other oxides is more remarkable. $NaCo_2O_4$ shows 100 μV/K at room temperature, while the layered Cu, Ni, and Mn oxides show very small thermopower of the order of 1-10 μV/K. Thus the most peculiar feature of the layered Co oxide is the unusually high thermopower.

10.5.2 Physics of the layered Co oxides

As an origin of the large thermopower, Koshibae, Tsutsui and Maekawa (2000) proposed an extended Heikes formula for transition-metal oxides written as

$$S = \frac{k_B}{C} \log \frac{g_A}{g_B} \frac{p}{1-p} \qquad (47)$$

where g_A and g_B are the degeneracy of the electron configuration of A and B ions, C is the charge difference between A and B ions, and p is the atomic content of the A ion. Since $k_B \log \frac{g_A}{g_B} \frac{p}{1-p}$ is equal to the entropy per carrier, Eq. (47) is a special case of Eq. (9).

Let us apply the above formula to $NaCo_2O_4$. Assuming that Na and O exist as Na^+ and O^{2-} in $NaCo_2O_4$, we expect that Co ions exists as Co^{3+} and Co^{4+} with a ratio of Co^{3+}:Co^{4+}=1:1. Then p for $NaCo_2O_4$ is equal to 0.5, and S for p=0.5 is simply reduced to $S = \frac{k_B}{C} \log \frac{g_A}{g_B}$. Magnetic measurements reveal that the Co^{4+} and Co^{3+} ions are in the low spin

state in $NaCo_2O_4$. As shown in the upper part of Fig. 10.11, the configuration of the low-spin-state Co^{3+} is $(t_{2g})^6$, whose entropy is zero. On the other hand, the low-spin-state Co^{4+} has a hole in the t_{2g} states, which is six-fold degenerate (two from spin and three from t_{2g} orbitals) to carry large entropy of $k_B\log 6$. Suppose electric conduction occurs by exchanging Co^{3+} and Co^{4+}, as is shown in the lower part of Fig. 10.11. Then a hole on Co^{4+} can carry a charge of $+e$ with entropy of $k_B\log 6$, which causes a large thermopower of $k_B\log 6/e$ (~150μV/K). This is very close to the high-temperature value of the thermopower. Note that carriers in degenerate semiconductors have no internal degrees of freedom: they can only carry entropy due to their kinetic energy. In this sense, a hole in $NaCo_2O_4$ can carry much larger entropy than degenerate semiconductors, which leads us a new design for thermoelectric materials.

Although Koshibae's theory has successfully explained the high-temperature limit thermopower of $NaCo_2O_4$, the remaining problem is not so simple. The thermopower of $NaCo_2O_4$ is 100 μV/K at 300 K, which is about 2/3 of $k_B\log 6$, which means that the large amount of entropy of $k_B\log 6$ in the high-temperature limit (~10^4 K) survives down to 10^2 K. We think it important that $NaCo_2O_4$ shows no structural, electric, and magnetic transitions from 2 to 1000 K. Usually various phase transitions occur in order to release an excess entropy per cites in the strongly correlated systems. Then, if all the phase transition were blocked, the large entropy would inevitably point to the conducting carriers (Terasaki 2002).

10.6 Summary and future prospects

In this chapter, we have briefly reviewed the thermoelectric phenomena and the thermoelectrics. Since thermoelectrics is a direct energy conversion between heat and electric power, it has various advantages. It can get some electric energy back from waste heat, and can cool materials without an exchange media like a freon gas. Thus this technology has attracted a renewed interest from the viewpoint of increasing needs for environment-friendly energy source. In the last decade, new thermoelectric materials have been searched extensively, some of which have better thermoelectric properties than the conventional thermoelectric materials.

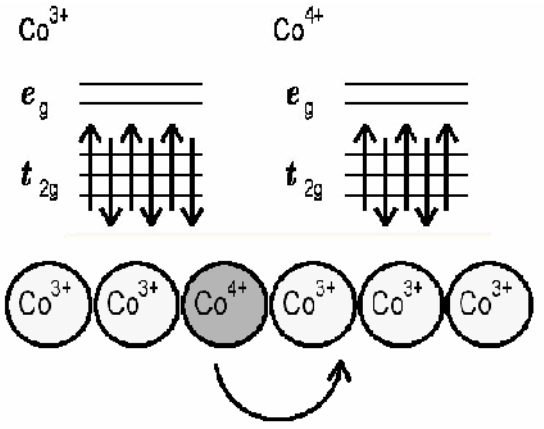

Figure 10.11 Electronic states of the Co ions, and the schematic picture of electric conduction in the layered Co oxides

From a viewpoint of basic science, the thermoelectric power is an entropy (or heat) carried by an electron. This is more or less controversial terminology, because the entropy and heat are a concept in the macroscopic world, whereas the electron is a concept in the microscopic world. Thus a new thermoelectric effect is lying near the boundary between microscopic and macroscopic worlds, which will give a new insight or direction to condensed matter science.

Acknowledgments

I would like to thank K. Matsubara, H. Anno, T. Caillat, C. Uher for fruitful discussion on thermal properties of skutterudites. Our work cited in this manuscript was partially supported by PRESTO and CREST projects of Japan Science and Technology Agency.

References

Anno H and Matsubara K (2000), *Recent Res. Devel. Applied Phys.*, 3, 47-61.

Ashcroft N W and Mermin N D (1976), *Solid State Physics*, Philadelphia, Saunders.

Caillat T, Borshchevsky A, and Fleurial J-P (1996), 'Properties of single crystalline semiconducting $CoSb_3$', J. Appl. Phys. 80, 4442-4449.

Callen H B (1985), *Thermodynamics and an introduction to thermostatistics* 2nd edition, Chapter 14, New York, John Wiley & Sons.

Chaikin P M and Beni G (1976), 'Thermopower in the correlated hopping regime', *Phys. Rev.*, B13, 647-651.

Chung D Y, Hogan T, Brazis P, Rocci-Lane M, Kannewurf C, Bastea M, Uher C, Kanatzidis M G (2000), '$CsBi_4Te_6$: A High-Performance Thermoelectric Material for Low-Temperature Applications', *Science*, 287, 1024-1027.

Fujita K, Mochida T, and Nakamura K (2001), 'High-temperature thermoelectric properties of $Na_xCoO_{2-\delta}$ single crystals', *Jpn. J. Appl. Phys.*, 40, 4644-4647.

Funahashi R, Matsubara I, Ikuta H, Takeuchi T, Mizutani U, and Sodeoka S (2000), 'An oxide single crystal with high thermoelectric performance in air', *Jpn. J. Appl. Phys.*, 39, L1127-1129.

Funahashi R and Matsubara I (2001), 'Thermoelectric properties of Pb- and Ca-doped $(Bi_2Sr_2O_4)_xCoO_2$ whiskers', *Appl. Phys. Lett.*, 79, 362-364.

Hébert S, Lambert S, Pelloquin D, and Maignan A (2001), 'Large thermopower in a metallic cobaltite: The layered Tl-Sr-Co-O misfit', *Phys. Rev.*, B 64, (2001), 172101.

Koshibae W, Tsutsui K and Maekawa S (2000), 'Thermopower in cobalt oxides', *Phys. Rev.*, B62, 6869-6872.

Koumoto K, Terasaki I and Murayama N (eds.) (2003), *Oxide Thermoelectrics*, Trivandrum, Research Signpost.

Maignan A, Hebert S, Pelloquin D, Michel C and Hejtmanek J (2002), 'Thermopower enhancement in misfit cobaltites', *Appl. Phys.*, 92, 1964-1967.

Mahan G D (1989), 'Figure of merit for thermoelectrics', *J. Appl. Phys.*, 65, 1578-1583.

Mahan G D (1998), 'Good thermoelectrics', *Solid State Phys.*, 51, 81-157.

Nolas G S, Cohn J L, Slack G A and Schujman S B (1998), 'Semiconducting Ge clathrates: Promising candidates for thermoelectric applications', *Appl. Phys. Lett.*, 73, 178-180.

Slack G A (1995), in '*CRC Handbook of Thermoelectrics*', edited by D. M. Rowe, Boca Raton FL, CRC Press, Chap. 34.

Sales B C, Mandrus D, Chakoumakos B C, Keppens V, and Thompson V R (1997), 'Filled skutterudite antimonides: Electron crystals and phonon glasses' *Phys. Rev.*, B56, 15081-15089.

Shikano M and Funahashi R (2003), 'Electrical and thermal properties of single-crystalline $(Ca_2CoO_3)_{0.7}CoO_2$ with a $Ca_3Co_4O_9$ structure', *Appl. Phys. Lett.*, 82, 1851-1853.

Terasaki I, Sasago Y and Uchinokura K (1997), 'Large thermoelectric power in $NaCo_2O_4$ in single crystals', *Phys. Rev.*, B56, R12685-12687.

Terasaki I, Tsukada I and Iguchi Y (2002), 'Impurity-induced transition and impurity-enhanced thermopower in the thermoelectric oxide $NaCo_{2-x}Cu_xO_4$' ,Phys. Rev., B65, 195106.

Tokura Y and Arima T (1990), 'New Classification Method for Layered Copper Oxide Compounds and Its Application to Design of New High Tc Superconductors', *Jpn. J. Appl. Phys.*, 29, 2388-2402.